

Universal Behavior of Highly Confined Heat Flow in Semiconductor Nanosystems: From Nanomeshes to Metalattices

Brendan McBennett, Albert Beardo,* Emma E. Nelson, Begoña Abad, Travis D. Frazer, Amitava Adak, Yuka Esashi, Baowen Li, Henry C. Kapteyn, Margaret M. Murnane, and Joshua L. Knobloch*



Cite This: *Nano Lett.* 2023, 23, 2129–2136



Read Online

ACCESS |

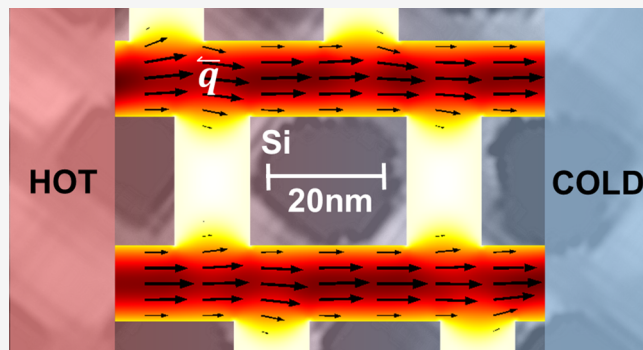
Metrics & More

Article Recommendations

Supporting Information

ABSTRACT: Nanostructuring on length scales corresponding to phonon mean free paths provides control over heat flow in semiconductors and makes it possible to engineer their thermal properties. However, the influence of boundaries limits the validity of bulk models, while first-principles calculations are too computationally expensive to model real devices. Here we use extreme ultraviolet beams to study phonon transport dynamics in a 3D nanostructured silicon *metalattice* with deep nanoscale feature size and observe dramatically reduced thermal conductivity relative to bulk. To explain this behavior, we develop a predictive theory wherein thermal conduction separates into a geometric *permeability* component and an intrinsic *viscous* contribution, arising from a new and universal effect of nanoscale confinement on phonon flow. Using experiments and atomistic simulations, we show that our theory applies to a general set of highly confined silicon nanosystems, from metalattices, nanomeshes, porous nanowires, to nanowire networks, of great interest for next-generation energy-efficient devices.

KEYWORDS: Nanoscale thermal transport, 3D phononic crystal, phonon hydrodynamics, Extreme ultraviolet scatterometry



While electrons and spins are readily manipulated with external fields, no equivalent tool exists for phonons, which are the sole heat carriers in semiconductors. This lack of control over phonons has impeded efforts to engineer energy-efficient devices with tailored thermal properties, including thermoelectrics and phononic analogues to electronic devices.¹ One promising means of influencing phonons is through nanoscale structuring, where the introduction of features smaller than the mean free paths (MFPs) for phonon–phonon collisions impedes thermal transport, thereby modifying the thermal conductivity and providing greater control over heat flow.²

Under highly confined heat transport conditions, phonons are usually assumed to be ballistic—implying that they travel between boundaries without internal collisions. Accordingly, the phonon MFPs are determined by the system size and geometry. Thermal conduction is commonly modeled in such situations using stochastic Monte Carlo solvers of the Boltzmann transport equation, wherein phonons with velocities and intrinsic scattering rates sampled from bulk *ab initio* calculations percolate through the nanoscale structure.³ This ballistic–stochastic approach has been applied extensively to explain dramatic reductions in thermal conductivity in 2D phononic crystals, consisting of periodic nanoscale voids in a crystalline background.^{4,5} However, geometric dependencies in

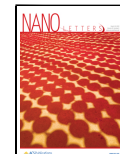
these models must be computed case-by-case, and thus extrapolation to newly available 3D nanostructured systems is nonintuitive and computationally challenging.^{6,7}

Ballistic simulations predict a ray-like propagation of phonons in analogy with photons.⁸ This contrasts with recent molecular dynamics (MD) investigations of energy flow profiles in nanowires,⁹ which show a Poiseuille-like flow reminiscent of hydrodynamics.^{10,11} These observations indicate the existence of a significant amount of phonon–phonon scattering and momentum diffusion at length scales much smaller than most of the bulk phonon MFPs, challenging the use of bulk phonon properties in nanoscale ballistic models.^{12,13} While hydrodynamic effects are known to be enhanced at low temperatures or in 2D materials, where most phonon–phonon collisions conserve momentum,^{14,15} increasing evidence suggests that they are also present at the nanoscale in semiconductors such as silicon—even at room temperature.^{16–19} Therefore, a complete understanding of the

Received: November 9, 2022

Revised: February 27, 2023

Published: March 7, 2023



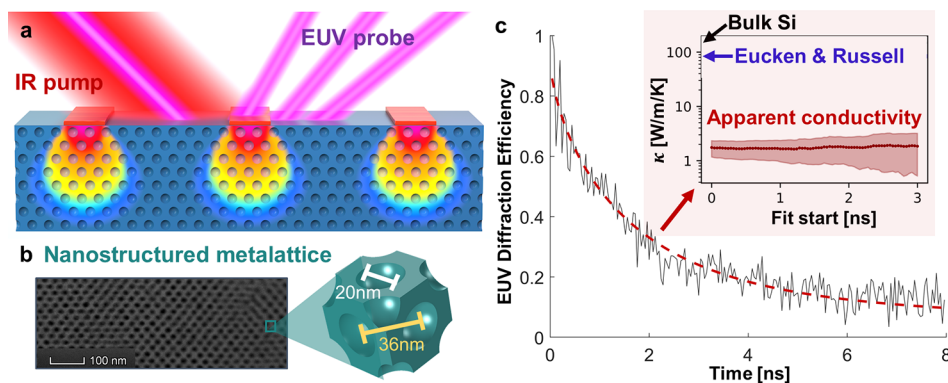


Figure 1. Observation of ultralow thermal conductivity in 3D silicon metalattices at room temperature. (a) Schematic of the experimental setup. A time-delayed EUV probe monitors the thermal relaxation of a nickel grating on the metalattice surface after excitation by an ultrafast infrared laser pump pulse. (b) Cross-sectional electron microscopy image of the metalattice structure. The approximately 500 nm thick metalattice film consists of crystalline silicon punctured by FCC-packed pores of 36 nm periodicity and approximately 20 nm diameter, resulting in a porosity of 0.385 ± 0.02 .²³ (c) An example experimental scan (gray) fit using Fourier's law (dashed red) with an ultralow thermal conductivity. The inset plots the bulk silicon conductivity (black), volume-reduced Eucken and Russell thermal conductivity (blue), and the apparent metalattice thermal conductivity (red), which is only 1% of the bulk. Note that, since the apparent thermal conductivity does not vary with fit start time, the observed dynamics can be captured within a Fourier framework, where the metalattice is treated as an effective medium.

breakdown of diffusive phonon transport in complex systems may require mesoscopic interpretations in analogy to fluid mechanics. Moreover, the degree to which heat dissipation through boundary scattering can be treated incoherently at the nanoscale remains unclear, since coherent effects modifying the phonon dispersion relations with respect to the bulk have been predicted and observed under some conditions.^{4,20–22} These contradictions contribute to the lack of a unified description of heat transport in nanostructured semiconductors, especially at the smallest length scales and in emerging 3D phononic crystals.⁶

In this work, we study highly confined heat flow in a 3D silicon phononic crystal “metalattice” at room temperature using time-resolved extreme ultraviolet (EUV) scatterometry. The metalattice periodicity is 36 nm, far below the average phonon mean free path in bulk silicon. We observe Fourier-like transport dynamics with an apparent thermal conductivity of only 1% of bulk. To explain these and a broad set of similar measurements on highly confined silicon nanosystems—including metalattices, nanomeshes, porous nanowires, and nanowire networks^{5,6,20}—we develop a predictive theory of heat flow in nanostructured silicon with dimensions far below the bulk phonon MFP. Through an analogy to the dynamics of rare gases in porous media, we decompose the thermal conductivity into permeability and viscosity components, where the former accounts for geometrical effects and the latter encompasses the intrinsic effect of nanoscale confinement on phonon flow and interactions. By comparing a broad set of experimental data with atomistic simulations, we uncover a universal relationship between viscosity and porosity, which yields a general analytical expression for thermal conductivity across highly confined 2D and 3D silicon nanosystems. This surprising and general finding suggests a fundamentally modified phase space for heat transport enabled by phonon-phonon interactions in nanostructured silicon. Moreover, the resulting analytical model provides a route to predict phonon transport in boundary-dominated nanosystems for next-generation energy-efficient devices, making it possible for the first time to represent them as effective media in engineering applications.

The silicon metalattice film studied here consists of a crystalline silicon background interrupted by periodic FCC-packed spherical voids of approximately 20 nm diameter and 36 nm periodicity, as shown in Figure 1(b). It is the identical sample investigated in ref 23, where its porosity and elastic properties were characterized in preparation for the present study. Details on the fabrication appear in refs 6 and 23 and Supporting Information (SI) section 1. We excite the metalattice film using an ultrafast infrared pump laser and then monitor its time-delayed surface deformation using an ultrafast 30 nm-wavelength EUV probe,^{24,25} as shown in Figure 1(a). A set of 1D periodic nanoscale nickel gratings are fabricated on the sample surface, to act as both absorbers for the infrared pump and a diffraction grating for the EUV probe. After excitation, the gratings relax by injecting energy across the nickel–silicon interface and into the metalattice film, as shown in Figure 1(c). Further details on the experimental technique can be found in SI section 2.

We model the thermoelastic response of the system using finite element methods and translate the simulated surface displacement to EUV diffraction efficiency, to directly compare with experimental data¹⁷ (details in SI section 3). Interestingly, the finite element simulations reveal that the transient relaxation of the metalattice can be accurately modeled, even at short time scales, using Fourier's law for the heat flux \vec{q} and the temperature T

$$\vec{q} = -\kappa \nabla T \quad (1a)$$

$$\nabla \cdot \vec{q} = -(1 - \phi) c_V \frac{\partial T}{\partial t} \quad (1b)$$

where c_V is the bulk silicon specific heat, κ is the apparent thermal conductivity of the effective medium representing the metalattice, and $\phi = 0.385 \pm 0.02$ is the metalattice porosity from ref 23. The appropriateness of the Fourier model is demonstrated in the inset to Figure 1(c), wherein the experimental data set shows no systematic dependence of fitted conductivity on fit start time. A time-dependent thermal conductivity is a hallmark of non-Fourier phonon transport,¹⁷ because it indicates a thermal relaxation incompatible with eq 1a, regardless of the assumed value of κ . The fits displayed in

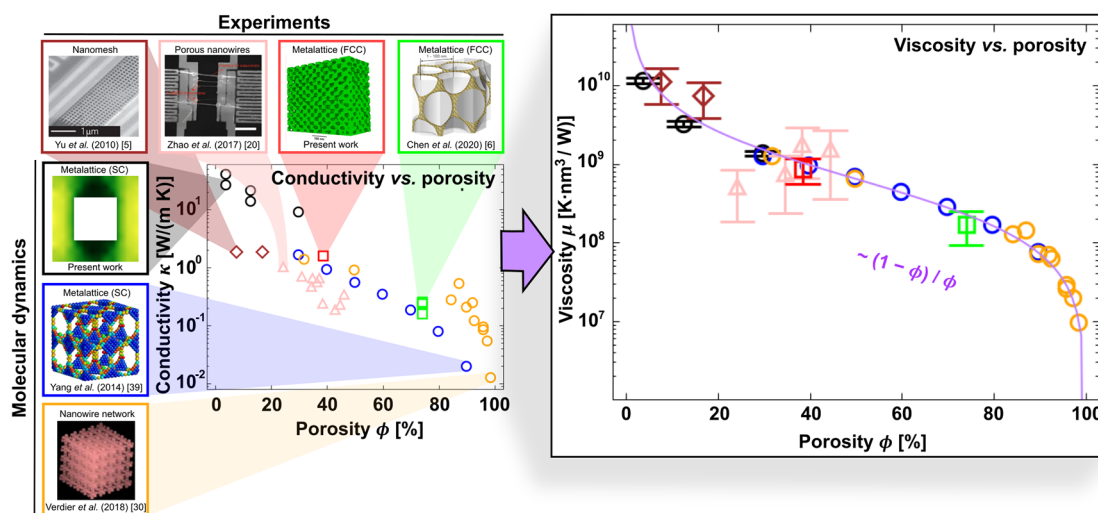


Figure 2. Universal scaling of viscosity with porosity in highly confined nanosystems. Left: Apparent thermal conductivity κ . Right: Viscosity μ from eq 4 as a function of nanostructured silicon system porosity. The viscosity captures the intrinsic phonon properties in nanostructured silicon systems regardless of their specific geometry and follows a universal trend. The theoretical results considered include new MD simulations of square-pore metalattices (black circles), along with previous MD simulations of circular-pore metalattices [blue circles (inset) - Reproduced from ref 39. Copyright 2014 ACS] and 3D nanowire networks [yellow circles (inset) - Reprinted with permission from ref 30. Copyright 2018 APS]. Experimental results considered include data on circular-pore FCC-packed metalattices from the present study (red square), a high-porosity metalattice with similar geometry from a previous study [green square (inset) - Reproduced from ref 6. Copyright 2020 ACS], along with previous data on 2D cylindrical-pore nanomeshes [brown diamonds (inset) - Reproduced from ref 5. Copyright 2010 Springer Nature] and porous nanowires [pink triangles (inset) - Reproduced from ref 20. Copyright 2017 WILEY-VCH Verlag GmbH]. In all experiments, phonon transport is confined in 3D to dimensions approximately 10% or less of the average phonon mean free path in bulk silicon. All details on the sample geometry and permeability calculations in each case appear in SI section 5C.

Figure 1(c) constrain the apparent metalattice thermal conductivity to $\kappa = 1.6 \pm 0.4$ W/mK (details in SI section 4), 2 orders of magnitude below the bulk crystalline value $\kappa_{\text{bulk}} = 149$ W/mK. Contrary to previous studies on bulk silicon,^{17,26} we observe no meaningful variation in the fitted conductivity with heater line width and periodicity. The quality of the fits indicates that explicit simulation of the pores along with complex transport equations beyond effective Fourier's law is unnecessary. However, the measurements cannot be explained by the classical volume reduction effect, as described in the models of Eucken $\kappa_{\text{Eucken}} = \kappa_{\text{bulk}}(1-\phi)/(1+(\phi/2)) = 77$ W/mK^{27,28} or Russell $\kappa_{\text{Russell}} = \kappa_{\text{bulk}}(1-\phi^{2/3})/(1-\phi^{2/3}+\phi) = 82$ W/mK²⁹ and shown in Figure 1(c). Therefore, a more fundamental explanation accounting for the interaction between the phonon population involved in the heat transport and the metalattice nanostructure is required.

To develop a comprehensive theory predicting the measured κ in both the metalattice and a broader class of highly confined nanostructured systems,^{5,20,30} we combine a phonon hydrodynamics framework³¹ and the theory of rarefied gas dynamics in porous media.^{32,33} Previous work has demonstrated that nanoscale size and frequency effects on heat transport in silicon can be modeled in terms of nonlocal and memory effects, as described by the Guyer–Krumhansl equation (GKE),³⁴ with *ab initio* geometry-independent coefficients.^{16,17,35,36} However, the predictive capabilities of this hydrodynamic-like approach are restricted to systems with dimensions sufficiently large compared to the average bulk phonon MFP,³⁷ since nanoscale confinement modifies the *ab initio* phonon properties used to determine the GKE coefficients.^{10,11} This excludes the present metalattice and a broader class of nanostructured silicon materials.

We overcome this limitation by using the similarities between the GKE and the Navier–Stokes equation for mass

transport in fluids. In analogy to Stokes flow in incompressible fluids at low Reynolds numbers, we first simplify the GKE by assuming that, in highly confined nanosystems, the thermal gradient is almost fully compensated by the viscous resistance described by the Laplacian term.³³ Here, a highly confined nanosystem refers to any crystalline semiconductor whose bulk average phonon MFP significantly exceeds the nanostructure length scale.

The resulting transport equation is a Stokes equation analogue in the absence of volume viscosity effects

$$\nabla T = \frac{l^2}{\kappa_{\text{GK}}} \nabla^2 \vec{q} \quad (2)$$

where κ_{GK} is the thermal conductivity appearing in the GKE and l is an averaged resistive MFP known as the nonlocal length. In the previous equation, we identify $\mu \equiv l^2/\kappa_{\text{GK}}$ as the dynamic phonon gas viscosity, which models the strength of the interaction between the pore walls and the phonon population.

Inside the metalattice, eq 2 can be further simplified in analogy to Darcy's law for fluid flow in porous media as

$$\nabla T = -\frac{\mu}{K} \vec{q} \quad (3)$$

where K is the metalattice permeability, which encompasses its geometrical properties. The permeability accounts for a nonzero heat flux, or slip heat flux, at the pore boundaries. This is analogous to the application of Darcy's law in rare gases, where collisions between fluid particles are scarce relative to momentum-destroying collisions with the boundaries.³⁸ Details on the derivation of the Darcy's law analogue from the GKE appear in SI section 5.

The appropriateness of eq 3 is validated by the success of the Fourier's law in eq 1a in modeling the experiment, allowing the identification

$$\kappa = \frac{K}{\mu} \quad (4)$$

The apparent thermal conductivity can thus be interpreted as a ratio between a permeability K , which only depends on geometry, and the viscosity μ , which is determined by the metalattice's averaged phonon dynamical properties.

This interpretation of the apparent conductivity enables the comparison of present and past experiments⁶ and MD simulations³⁹ of metalattices with varying pore distributions, sizes, shapes, and periodicities. Remarkably, it also enables comparison across a broad class of nanostructured silicon materials including 3D interconnected wire networks,³⁰ nanomeshes,⁵ and porous nanowires.²⁰ The model is only valid for sufficiently constrained systems, with characteristic sizes of a few tens of nanometers. It cannot be extended to larger-scale structured materials (e.g., refs 4 and 40) at room temperature due to the breakdown of the Stokes regime assumption neglecting the heat flux contribution in the GKE (details in SI section 6B).

In addition to quantifying κ in the different systems, it is necessary to characterize the permeability K —a purely geometrical quantity—to extract the phonon viscosity μ . We follow the Kozeny–Carman derivation,³² including the Klinkenberg quasiballistic correction and assuming diffusive phonon-boundary collisions³⁸ (see SI section 5), to obtain the following expression

$$K = \frac{d^2 \Psi^2 (1 - \phi)^3}{24 \Gamma^2 \phi^2} \quad (5)$$

where d is the average empty pore diameter, Ψ is the sphericity of the pores (i.e., the surface area ratio of the ideal spherical pore to the actual pore), and Γ is the tortuosity (i.e., the ratio of the average length of a heat flux streamline to the distance between its ends). Then, using eqs 4 and 5, one can characterize the phonon viscosity μ in systems with a 3D distribution of empty pores using only the measured apparent conductivity κ and the average geometric properties (ϕ, d, Ψ, Γ). Expression 5 can be easily adapted to characterize permeability in a variety of geometries beyond metalattices. For example, a nanowire network can be modeled as a porous medium, with porosity and pore size defined in terms of wire diameter and periodicity, while, for nanomeshes, the permeability can be expressed in terms of a 2D distribution of cylindrical pores in a thin film (see SI section 5B and eq S24). The sphericity parameter Ψ can be characterized via electron microscopy to model imperfectly spherical pores in experiments, or used to account for other pore shapes such as cubes.

In Figure 2, we show the apparent conductivity κ and the viscosity μ as functions of porosity for new and previous MD simulations in metalattices³⁹ and 3D nanowire networks,³⁰ along with present and past experimental results in metalattices,⁶ nanomeshes,⁵ and porous nanowires²⁰ (details in SI sections 5C and 6). The thermal conductivity κ at a given porosity depends strongly on specific geometrical details such as pore size, shape, and distribution. Conversely, the viscosity μ depends solely on porosity across all nanostructured systems in both experiments and MD simulations. More precisely, the

viscosity scales as $(1 - \phi)/\phi$, the ratio of the available to nonavailable volume for heat transport. Combining this universal scaling with eqs 4 and 5, one obtains an analytical expression for the apparent thermal conductivity in nanostructured silicon systems with feature sizes far below the average bulk phonon MFP.

Since the intrinsic phonon properties are seen to depend primarily on nanosystem porosity, regardless of the specific geometry, the variations in thermal conductivity at a given porosity observed in Figure 2 can be attributed to the permeability K , which only depends on geometry. Permeability not only accounts for the classical volume reduction effect but also captures nanoscale geometrical effects, and it can be used to reinterpret correlations between thermal conductivities and geometric descriptors observed in the literature.^{41–44} For example, the differences between the permeability and the surface-to-volume ratio justify why the latter is not a general proxy for thermal conductivity in nanostructured systems.⁵ The influence of the neck size on the permeability can be investigated by identifying the neck size with the channel diameter D and using the 3D geometrical relation, $D = 2(1 - \phi)\Psi d/3\phi$ in eq 5, as discussed in SI section 5A. The corresponding 2D geometrical relation can be found in SI section 5B and eq S23. The neck size has been shown to be a good indicator of the effects of nanostructuring on thermal conductivity,^{7,45} and the present model agrees with previous findings that thermal conductivity varies as the square of neck size under highly confined transport conditions.⁴⁴ Moreover, some purely geometrical effects commonly invoked in phononic crystals like pore anisotropy,⁴⁶ backscattering,⁴⁰ or surface disorder⁴⁷ can be related to the permeability. Pore anisotropy might be described by the tortuosity Γ , and surface disorder may modify the slip flux boundary condition, which determines the numerical factor in eq 5 (details in SI section 5). However, it is worth noting that it was not necessary to characterize the influence of these effects when calculating each sample's permeability in order to uncover the universal scaling of μ , suggesting that these are not the key mechanisms distinguishing the different cases considered. Finally, the resistive effect associated with backscattering in ballistic interpretations is quantified by the geometrical parameters appearing in K , which depend on the size and frequency of channels orthogonal to the thermal gradient.

The universal relationship between viscosity and porosity is reminiscent of a non-Newtonian fluid,⁴⁸ and provides insight into the intrinsic mechanisms influencing phonon transport in highly confined nanosystems. According to kinetic theory,¹⁶ the thermal conductivity κ_{GK} and nonlocal length l are related to the phonon MFP Λ as $\kappa_{\text{GK}} \propto \Lambda$ and $l^2 \propto \Lambda^2$, respectively. This implies that $\mu \propto \Lambda$. However, in Figure 2, systems with the same porosities but different neck sizes are shown to have the same viscosity. In line with previous work, this contradicts the ballistic assumption wherein Λ is determined by the neck size and challenges the applicability of the standard Matthiessen's rule in estimating scattering times.^{49,50} In the fully ballistic limit where porosity approaches 100%, μ declines to zero. However, we observe that, even at high porosities above 80% ($\phi = 0.8$), MD simulation geometries with dramatically different values of κ collapse to the same value of μ , indicating that a hydrodynamic-like description of the phonon flow can be extended to extremely constrained systems. These results suggest that the phonon distribution evolves collectively under nanoscale confinement, and should

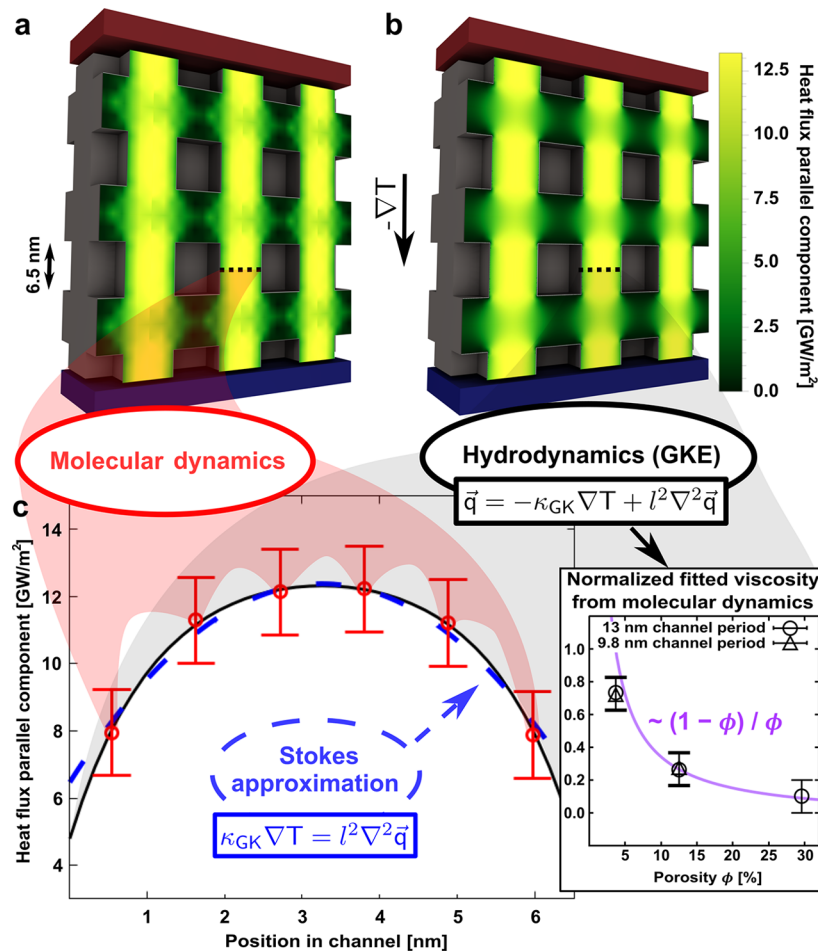


Figure 3. Fluid-like heat flow in highly confined nanosystems. Parabolic heat flux profiles in 3D metatlattices are predicted by both molecular dynamics simulations and hydrodynamic simulations, confirming the universal viscosity scaling. (a) Heat flux profile according to an MD simulation of a metatlattice with cubic pores (see SI section 6). The channel spacing is 13 nm, and the pore side length is 6.5 nm. The imposed temperature difference between the ends of the system is 20 K. (b) Heat flux profile fitted to the same geometry using the GKE and appropriate parameter values for l and κ_{GK} . (c) Heat flux profile along a cross-section between two contiguous pores according to MD (dots) and the GKE fit (solid black line). The Stokes fit (dashed blue line) can locally reproduce the flux in the passage between the pores. The inset plots the viscosity $\mu = l^2 / \kappa_{\text{GK}}$ obtained from the GKE fits for channel periods of 13 nm (circles) or 9.8 nm (triangles). It follows the same scaling with porosity as observed in experiments.

be characterized by averaged phonon properties including l , κ_{GK} , and μ , rather than multiscale descriptions where each phonon mode evolves independently with a distinct MFP. This perspective is consistent with recent electron transport experiments, where current profiles exhibit hydrodynamic-like vortices at low temperatures.⁵¹ Since momentum-conserving electron–electron collisions are scarce under these conditions, the observed behavior is instead induced by nanoscale confinement, in analogy to the emergence of phonon hydrodynamics in silicon nanosystems.

To investigate the universal scaling of μ , we directly quantify its magnitude using local heat flux profiles calculated from atomistic simulations. In Figure 3, we show the steady-state heat flux profile in a 3D metatlattice as obtained from MD simulations (details in SI section 6). We then fit the atomistic profiles using the steady-state GKE

$$\vec{q} = -\kappa_{\text{GK}} \nabla T + l^2 \nabla^2 \vec{q} \quad (6)$$

with appropriate values for κ_{GK} and l , and slip boundary conditions. The excellent fit quality further validates the use of hydrodynamic-like modeling to describe heat transport in

highly confined nanosystems. The Poiseuille-like profiles obtained in MD are incompatible not only with the exponential profiles predicted by the Fuchs–Sondheimer approximation to the Boltzmann transport equation¹¹ but also with more general ballistic descriptions using the bulk MFP spectrum.⁸ The viscosity fit with the steady-state GKE $\mu = l^2 / \kappa_{\text{GK}}$ follows the same scaling with porosity obtained from experiments using κ and K in eq 5. The observed decrease in μ with increasing porosity is due to a reduction in the size of strongly correlated heat flux regions surrounding the boundaries, whose extent is described by l . However, the conductivity parameter κ_{GK} is also slightly reduced. For fixed porosity, both l and κ_{GK} increase when increasing the pore spacing, but the resulting viscosity μ remains the same. In Figure 3, we also show that the Stokes approximation in eq 2 can fit the local heat flux profile in the passages between contiguous pores, as required in the Darcy’s law derivation. However, the Stokes approximation is not sufficient to predict the complete heat flux profile in MD simulations, including the complex pore boundaries (details on the GKE and Stokes fits in SI section 6B).

Since the volume reduction effect and the geometrical influence of the boundaries on thermal conductivity are included in the permeability, the viscosity μ might be related to intrinsic phonon properties and the emergence of coherent or incoherent phonon effects in nanosystems. For example, previous work experimentally observed elastic softening leading to reduced phonon velocities with increasing porosity, regardless of the specific geometric details.^{13,20} Elastic softening is not governed by the permeability and may influence the relationship between viscosity and porosity uncovered in Figure 2. Another possible source of variation in μ is the hypothetical presence of amorphous layers surrounding the pores in the sample, which are not considered in the Figure 2 MD data. Their presence might also reduce heat flux in the crystalline channels, which would result in an increased viscosity.^{11,52} Moreover, we find that viscosity is independent of disorder in the nanostructured system; e.g., the periodically arranged 3D metalattices display the same viscosity as the randomly distributed pores in the nanowires. Hence, coherent interference effects previously reported in periodically structured silicon systems at very low temperatures^{21,53} are negligible in the mainly room temperature experiments and simulations considered here. Finally, previous work detected the localization of phonon modes within metalattices at very high porosities,³⁹ which directly influences the total contribution of the phonon population to l^2 , κ_{GK} , and μ . A deeper understanding of the universal behavior uncovered here might require relating these average phonon properties with the dispersion relations in nanostructured silicon systems or with the modification of the phonon–phonon scattering rates in nanostructured systems relative to bulk.⁵⁴

In conclusion, we show that it is possible to use an effective medium theory with a Fourier relation to model heat transport in 3D metalattices and other highly confined silicon nanosystems. In contrast to a ballistic interpretation where phonon modes evolve independently, the present approach stems from an analogy to rarefied fluid flow in porous media, motivated by Poiseuille-like heat flux profiles observed in atomistic simulations of nanoscale channels. In highly confined nanosystems, thermal conduction separates into a permeability component, which captures the geometrical effect of complex structures, and a viscosity component related to the intrinsic phonon properties in the nanosystem environment. Variations in thermal conductivity between experiments or MD simulations at constant porosity can be attributed to the permeability, whereas viscosity depends solely on porosity and varies universally as $(1 - \phi)/\phi$. This leads to an analytical description of thermal conduction and suggests that the viscosity is the appropriate metric for exploring the modification of the phonon dispersion relations and scattering rates in semiconductor nanosystems beyond the ballistic interpretation. In general, these ideas might apply to describe the transport of other particles beyond phonons, where hydrodynamic signatures emerge in the presence of slowly evolving magnitudes that violate the local equilibrium assumption.^{55–57}

■ ASSOCIATED CONTENT

SI Supporting Information

The Supporting Information is available free of charge at <https://pubs.acs.org/doi/10.1021/acs.nanolett.2c04419>.

Metalattice fabrication, sphericity characterization, EUV scatterometry measurements, finite element model and thermal conductivity fitting, Darcy's law derivation and application to various geometries, and molecular dynamics simulations ([PDF](#))

■ AUTHOR INFORMATION

Corresponding Authors

Albert Beardo – Department of Physics, JILA, and STROBE NSF Science and Technology Center, University of Colorado and NIST, Boulder, Colorado 80309, United States;  orcid.org/0000-0003-1889-1588; Email: albert.beardo@colorado.edu

Joshua L. Knobloch – Department of Physics, JILA, and STROBE NSF Science and Technology Center, University of Colorado and NIST, Boulder, Colorado 80309, United States;  orcid.org/0000-0002-4086-3746; Email: joshua.knobloch@colorado.edu

Authors

Brendan McBennett – Department of Physics, JILA, and STROBE NSF Science and Technology Center, University of Colorado and NIST, Boulder, Colorado 80309, United States;  orcid.org/0000-0001-7947-6551

Emma E. Nelson – Department of Physics, JILA, and STROBE NSF Science and Technology Center, University of Colorado and NIST, Boulder, Colorado 80309, United States;  orcid.org/0000-0003-4336-3242

Begoña Abad – Department of Physics, JILA, and STROBE NSF Science and Technology Center, University of Colorado and NIST, Boulder, Colorado 80309, United States; Present Address: Physics Department, University of Basel, Klingelbergstrasse 82, CH-4056 Basel, Switzerland;  orcid.org/0000-0001-7589-7973

Travis D. Frazer – Department of Physics, JILA, and STROBE NSF Science and Technology Center, University of Colorado and NIST, Boulder, Colorado 80309, United States;  orcid.org/0000-0002-5162-4230

Amitava Adak – Department of Physics, JILA, and STROBE NSF Science and Technology Center, University of Colorado and NIST, Boulder, Colorado 80309, United States; Present Address: Department of Physics, IIT (ISM) Dhanbad, Jharkhand 826004, India;  orcid.org/0000-0003-0687-2830

Yuka Esashi – Department of Physics, JILA, and STROBE NSF Science and Technology Center, University of Colorado and NIST, Boulder, Colorado 80309, United States

Baowen Li – Department of Materials Science and Engineering, Department of Physics, Southern University of Science and Technology, Shenzhen 518055, PR China; Department of Mechanical Engineering, Department of Physics, University of Colorado, Boulder, Colorado 80309, United States;  orcid.org/0000-0002-8728-520X

Henry C. Kapteyn – Department of Physics, JILA, and STROBE NSF Science and Technology Center, University of Colorado and NIST, Boulder, Colorado 80309, United States;  orcid.org/0000-0001-8386-6317

Margaret M. Murnane – Department of Physics, JILA, and STROBE NSF Science and Technology Center, University of Colorado and NIST, Boulder, Colorado 80309, United States

Complete contact information is available at:

<https://pubs.acs.org/10.1021/acs.nanolett.2c04419>

Notes

The authors declare the following competing financial interest(s): Henry Kapteyn is partially employed by KM Labs, the company which manufactured the Ti:sapphire amplifier used in this work.

ACKNOWLEDGMENTS

The authors gratefully acknowledge support from the STROBE National Science Foundation Science & Technology Center, Grant No. DMR-1548924. A.B. acknowledges support from the Spanish Ministry of Universities through a Margarita Salas fellowship funded by the European Union - NextGenerationEU. This work utilized the Alpine high performance computing resource at the University of Colorado Boulder. Alpine is jointly funded by the University of Colorado Boulder, the University of Colorado Anschutz, and Colorado State University. The authors would also like to acknowledge Dr. Guimei Zhu for her proofing of the manuscript and Steven Burrows for assistance designing Figure 1(a).

REFERENCES

- (1) Li, N.; Ren, J.; Wang, L.; Zhang, G.; Hänggi, P.; Li, B. Colloquium: Phononics: Manipulating heat flow with electronic analogs and beyond. *Rev. Mod. Phys.* **2012**, *84*, 1045–1066.
- (2) Li, Y.; Li, W.; Han, T.; Zheng, X.; Li, B.; Fan, S.; Qiu, C.-W. Transforming heat transfer with thermal metamaterials and devices. *Nature Review Materials* **2021**, *6*, 488–507.
- (3) Hao, Q.; Chen, G.; Jeng, M.-S. Frequency-dependent Monte Carlo simulations of phonon transport in two-dimensional porous silicon with aligned pores. *J. Appl. Phys.* **2009**, *106*, 114321.
- (4) Hopkins, P. E.; Reinke, C. M.; Su, M. F.; Olsson, R. H.; Shaner, E. A.; Leseman, Z. C.; Serrano, J. R.; Phinney, L. M.; El-Kady, I. Reduction in the thermal conductivity of single crystalline silicon by phononic crystal patterning. *Nano Lett.* **2011**, *11* (1), 107–112.
- (5) Yu, J.-K.; Mitrovic, S.; Tham, D.; Varghese, J.; Heath, J. R. Reduction of thermal conductivity in phononic nanomesh structures. *Nature Nanotechnology* **2010**, *5*, 718–721.
- (6) Chen, W.; Talreja, D.; Eichfeld, D.; Mahale, P.; Nova, N. N.; Cheng, H. Y.; Russell, J. L.; Yu, S.-Y.; Poilvert, N.; Mahan, G.; Mohney, S. E.; Crespi, V. H.; Mallouk, T. E.; Badding, J. V.; Foley, B.; Gopalan, V.; Dabo, I. Achieving minimal heat conductivity by ballistic confinement in phononic metalattices. *ACS Nano* **2020**, *14* (4), 4235–4243.
- (7) Nomura, M.; Anufriev, R.; Zhang, Z.; Maire, J.; Guo, Y.; Yanagisawa, R.; Volz, S. Review of thermal transport in phononic crystals. *Materials Today Physics* **2022**, *22*, 100613.
- (8) Anufriev, R.; Ramiere, A.; Maire, J.; Nomura, M. Heat guiding and focusing using ballistic phonon transport in phononic nanostructures. *Nat. Commun.* **2017**, *8*, 15505.
- (9) Verdier, M.; Han, Y.; Lacroix, D.; Chapuis, P.-O.; Termentzidis, K. Radial dependence of thermal transport in silicon nanowires. *Journal of Physics: Materials* **2019**, *2*, 015002.
- (10) Melis, C.; Rurali, R.; Cartoixa, X.; Alvarez, F. X. Indications of phonon hydrodynamics in telescopic silicon nanowires. *Phys. Rev. Applied* **2019**, *11*, 054059.
- (11) Desmarchelier, P.; Beardo, A.; Alvarez, F. X.; Tangy, A.; Termentzidis, K. Atomistic evidence of hydrodynamic heat transfer in nanowires. *Int. J. Heat Mass Transfer* **2022**, *194*, 123003.
- (12) Jain, A.; Yu, Y.-J.; McGaughey, A. J. H. Phonon transport in periodic silicon nanoporous films with feature sizes greater than 100 nm. *Phys. Rev. B* **2013**, *87*, 195301.
- (13) Takahashi, K.; Fujikane, M.; Liao, Y.; Kashiwagi, M.; Kawasaki, T.; Tambo, N.; Ju, S.; Naito, Y.; Shiomi, J. Elastic inhomogeneity and anomalous thermal transport in ultrafine Si phononic crystals. *Nano Energy* **2020**, *71*, 104581.
- (14) Cepellotti, A.; Fugallo, G.; Paulatto, L.; Lazzeri, M.; Mauri, F.; Marzari, N. Phonon hydrodynamics in two-dimensional materials. *Nat. Commun.* **2015**, *6*, 6400.
- (15) Lee, S.; Broido, D.; Esfarjani, K.; Chen, G. Hydrodynamic phonon transport in suspended graphene. *Nature Communication* **2015**, *6*, 6290.
- (16) Sendra, L.; Beardo, A.; Torres, P.; Bafaluy, J.; Alvarez, F. X.; Camacho, J. Derivation of a hydrodynamic heat equation from the phonon Boltzmann equation for general semiconductors. *Phys. Rev. B* **2021**, *103*, L140301.
- (17) Beardo, A.; Knobloch, J. L.; Sendra, L.; Bafaluy, J.; Frazer, T. D.; Chao, W.; Hernandez-Charpak, J. N.; Kapteyn, H. C.; Abad, B.; Murnane, M. M.; Alvarez, F. X.; Camacho, J. A general and predictive understanding of thermal transport from 1D- and 2D-confined nanostructures: Theory and experiment. *ACS Nano* **2021**, *15* (8), 13019–13030.
- (18) Guo, Y.; Wang, M. Phonon hydrodynamics for nanoscale heat transport at ordinary temperatures. *Phys. Rev. B* **2018**, *97*, 035421.
- (19) Zhou, Y.; Zhang, X.; Hu, M. Nonmonotonic diameter dependence of thermal conductivity of extremely thin Si nanowires: Competition between hydrodynamic phonon flow and boundary scattering. *Nano Lett.* **2017**, *17*, 1269–1276.
- (20) Zhao, Y.; Yang, L.; Kong, L.; Nai, M. H.; Liu, D.; Wu, J.; Liu, Y.; Chiam, S. Y.; Chim, W. K.; Lim, C. T.; Li, B.; Thong, J. T. L.; Hippalgaonkar, K. Ultralow thermal conductivity of single-crystalline porous silicon nanowires. *Adv. Funct. Mater.* **2017**, *27* (40), 1702824.
- (21) Maire, J.; Anufriev, R.; Yanagisawa, R.; Ramiere, A.; Volz, S.; Nomura, M. Heat conduction tuning by wave nature of phonons. *Science Advances* **2017**, *3* (8), e1700027.
- (22) Davis, B. L.; Hussein, M. I. Nanophononic metamaterial: Thermal conductivity reduction by local resonance. *Phys. Rev. Lett.* **2014**, *112*, 055505.
- (23) Knobloch, J. L.; McBennett, B.; Bevis, C. S.; Yazdi, S.; Frazer, T. D.; Adak, A.; Nelson, E. E.; Hernández-Charpak, J. N.; Cheng, H. Y.; Grede, A. J.; Mahale, P.; Nova, N. N.; Giebink, N. C.; Mallouk, T. E.; Badding, J. V.; Kapteyn, H. C.; Abad, B.; Murnane, M. M. Structural and elastic properties of empty-pore metalattices extracted via nondestructive coherent extreme UV scatterometry and electron tomography. *ACS Appl. Mater. Interfaces* **2022**, *14*, 41316–41327.
- (24) Rundquist, A.; Durfee, C. G.; Chang, Z.; Herne, C.; Backus, S.; Murnane, M. M.; Kapteyn, H. C. Phase-matched generation of coherent soft X-rays. *Science* **1998**, *280* (5368), 1412–1415.
- (25) Tobey, R. I.; Siemens, M. E.; Cohen, O.; Murnane, M. M.; Kapteyn, H. C.; Nelson, K. A. Ultrafast extreme ultraviolet holography: dynamic monitoring of surface deformation. *Opt. Lett.* **2007**, *32*, 286–288.
- (26) Hoogeboom-Pot, K. M.; Hernandez-Charpak, J. N.; Gu, X.; Frazer, T. D.; Anderson, E. H.; Chao, W.; Falcone, R. W.; Yang, R.; Murnane, M. M.; Kapteyn, H. C.; Nardi, D. A new regime of nanoscale thermal transport: Collective diffusion increases dissipation efficiency. *Proc. Natl. Acad. Sci. U. S. A.* **2015**, *112* (16), 4846–4851.
- (27) Song, D.; Chen, G. Thermal conductivity of periodic microporous silicon films. *Appl. Phys. Lett.* **2004**, *84*, 687–689.
- (28) Wang, J.; Carson, J. K.; North, M. F.; Cleland, D. J. A new approach to modelling the effective thermal conductivity of heterogeneous materials. *Int. J. Heat Mass Transfer* **2006**, *49* (17), 3075–3083.
- (29) Russell, H. W. Principles of heat flow in porous insulators. *J. Am. Ceram. Soc.* **1935**, *18*, 1–5.
- (30) Verdier, M.; Lacroix, D.; Termentzidis, K. Thermal transport in two- and three-dimensional nanowire networks. *Phys. Rev. B* **2018**, *98*, 155434.
- (31) Guo, Y.; Wang, M. Phonon hydrodynamics and its applications in nanoscale heat transport. *Phys. Rep.* **2015**, *S95*, 1–44.
- (32) Carman, P. C. *Flow of gases through porous media*; Academic Press Inc. Publishers: New York, 1956.
- (33) Alvarez, F. X.; Jou, D.; Sellitto, A. Pore-size dependence of the thermal conductivity of porous silicon: A phonon hydrodynamic approach. *Appl. Phys. Lett.* **2010**, *97*, 033103.

- (34) Guyer, R. A.; Krumhansl, J. A. Solution of the linearized phonon Boltzmann equation. *Phys. Rev.* **1966**, *148*, 766–778.
- (35) Ruiz-Clavijo, A.; Caballero-Calero, O.; Manzano, C. V.; Maeder, X.; Beardo, A.; Cartoixà, X.; Alvarez, F. X.; Martín-González, M. 3d bi₂te₃ interconnected nanowire networks to increase thermoelectric efficiency. *ACS Applied Energy Materials* **2021**, *4*, 13556.
- (36) Xiang, Z.; Jiang, P.; Yang, R. Time-domain thermoreflectance (TDTR) data analysis using phonon hydrodynamic model. *J. Appl. Phys.* **2022**, *132*, 205104.
- (37) Beardo, A.; Calvo-Schwarzwälder, M.; Camacho, J.; Myers, T.; Torres, P.; Sendra, L.; Alvarez, F.; Bafaluy, J. Hydrodynamic heat transport in compact and holey silicon thin films. *Phys. Rev. Applied* **2019**, *11*, 034003.
- (38) Klinkenberg, L. The permeability of porous media to liquids and gases. *Drilling and Production Practice* **1941**, *41*, 200.
- (39) Yang, L.; Yang, N.; Li, B. Extreme low thermal conductivity in nanoscale 3D Si phononic crystal with spherical pores. *Nano Lett.* **2014**, *14* (4), 1734–1738.
- (40) Lee, J.; Lee, W.; Wehmeyer, G.; Dhuey, S.; Olynick, D. L.; Cabrini, S.; Dames, C.; Urban, J. J.; Yang, P. Investigation of phonon coherence and backscattering using silicon nanomeshes. *Nat. Commun.* **2017**, *8*, 14054.
- (41) Zianni, X.; Jean, V.; Termentzidis, K.; Lacroix, D. Scaling behavior of the thermal conductivity of width-modulated nanowires and nanofilms for heat transfer control at the nanoscale. *Nanotechnology* **2014**, *25*, 465402.
- (42) Wei, H.; Bao, H.; Ruan, X. Machine learning prediction of thermal transport in porous media with physics-based descriptors. *Int. J. Heat Mass Transfer* **2020**, *160*, 120176.
- (43) Hahn, K. R.; Melis, C.; Colombo, L. Thermal conduction and rectification phenomena in nanoporous silicon membranes. *Phys. Chem. Chem. Phys.* **2022**, *24*, 13625–13632.
- (44) Lim, J.; Wang, H.-T.; Tang, J.; Andrews, S. C.; So, H.; Lee, J.; Lee, D. H.; Russell, T. P.; Yang, P. Simultaneous thermoelectric property measurement and incoherent phonon transport in holey silicon. *ACS Nano* **2016**, *10* (1), 124–132.
- (45) Anufriev, R.; Maire, J.; Nomura, M. Reduction of thermal conductivity by surface scattering of phonons in periodic silicon nanostructures. *Phys. Rev. B* **2016**, *93*, 045411.
- (46) Ferrando-Villalba, P.; D'Ortenzi, L.; Dalkiranis, G. G.; Cara, E.; Lopeandia, A. F.; Abad, L.; Rurali, R.; Cartoixà, X.; De Leo, N.; Saghi, Z.; Jacob, M.; Gambacorti, N.; Boarino, L.; Rodríguez-Viejo, J. Impact of pore anisotropy on the thermal conductivity of porous Si nanowires. *Sci. Rep.* **2018**, *8*, 12796.
- (47) Martin, P.; Aksamija, Z.; Pop, E.; Ravaioli, U. Impact of phonon-surface roughness scattering on thermal conductivity of thin Si nanowires. *Phys. Rev. Lett.* **2009**, *102*, 125503.
- (48) Chhabra, R. P. *Non-Newtonian Fluids: An Introduction*; Springer: New York, 2010; pp 3–34.
- (49) Cartoixà, X.; Dettori, R.; Melis, C.; Colombo, L.; Rurali, R. Thermal transport in porous Si nanowires from approach-to-equilibrium molecular dynamics calculations. *Appl. Phys. Lett.* **2016**, *109*, 013107.
- (50) Hosseini, S. A.; Davies, A.; Dickey, I.; Neophytou, N.; Greaney, P. A.; de Sousa Oliveira, L. Super-suppression of long phonon mean-free-paths in nano-engineered Si due to heat current anticorrelations. *Materials Today Physics* **2022**, *27*, 100719.
- (51) Aharon-Steinberg, A.; Völk, T.; Kaplan, A.; Pariari, A. K.; Roy, I.; Holder, I.; Wolf, Y.; Meltzer, A. Y.; Myasoedov, Y.; Huber, M. E.; Yan, B.; Falkovich, G.; Levitov, L. S.; Hücker, M.; Zeldov, E. Direct observation of vortices in an electron fluid. *Nature* **2022**, *607*, 74–80.
- (52) Lysenko, V.; Perichon, S.; Remaki, B.; Barbier, D.; Champagnon, B. Thermal conductivity of thick meso-porous silicon layers by micro-Raman scattering. *J. Appl. Phys.* **1999**, *86*, 6841.
- (53) Zen, N.; Puurtinen, T. A.; Isotalo, T. J.; Chaudhuri, S.; Maasilta, I. J. Engineering thermal conductance using a two-dimensional phononic crystal. *Nat. Commun.* **2014**, *5*, 3435.
- (54) Honarvar, H.; Knobloch, J. L.; Frazer, T. D.; Abad, B.; McBennett, B.; Hussein, M. I.; Kapteyn, H. C.; Murnane, M. M.; Hernandez-Charpak, J. N. Directional thermal channeling: A phenomenon triggered by tight packing of heat sources. *Proc. Natl. Acad. Sci. U. S. A.* **2021**, *118* (40), e2109056118.
- (55) Varnavides, G.; Jermyn, A. S.; Anikeeva, P.; Felser, C.; Narang, P. Electron hydrodynamics in anisotropic materials. *Nat. Commun.* **2020**, *11*, 4710.
- (56) Cheung, M. C. M.; Rempel, M.; Chintzoglou, G.; Chen, F.; Testa, P.; Martínez-Sykora, J.; Sainz Dalda, A.; DeRosa, M. L.; Malanushenko, A.; Hansteen, V.; De Pontieu, B.; Carlsson, M.; Gudiksen, B.; McIntosh, S. W. A comprehensive three-dimensional radiative magnetohydrodynamic simulation of a solar flare. *Nature Astronomy* **2019**, *3*, 160–166.
- (57) Gromov, A.; Lucas, A.; Nandkishore, R. M. Fracton hydrodynamics. *Phys. Rev. Research* **2020**, *2*, 033124.

□ Recommended by ACS

Quantifying the Spatial Distribution of Radiative Heat Transfer in Subwavelength Planar Nanostructures

Ayan Majumder, Edgar Meyhofer, et al.

APRIL 03, 2023
ACS PHOTONICS

READ ▶

Observation of Negative Effective Thermal Diffusion in Gold Films

Alexander Block, Yonatan Sivan, et al.

MARCH 28, 2023
ACS PHOTONICS

READ ▶

Experimental Evidence of Superdiffusive Thermal Transport in Si_{0.4}Ge_{0.6} Thin Films

Fengju Yao, Dongyan Xu, et al.

SEPTEMBER 02, 2022
NANO LETTERS

READ ▶

Multitemperature Modeling of Thermal Transport across a Au–GaN Interface from *Ab Initio* Calculations

Zhen Tong, Thomas Frauenheim, et al.

AUGUST 18, 2022
ACS APPLIED ELECTRONIC MATERIALS

READ ▶

Get More Suggestions >